SUPPORTING INFORMATION

Determination of Ion Atmosphere Effects on the Nucleic Acid Electrostatic Potential and Ligand Association Using AH^+•C Wobble Formation in Double-stranded DNA

Benjamin E. Allred[1], Magdalena Gebala[1], Daniel Herschlag[1,2,3]*

[1]Department of Biochemistry, Stanford University, Stanford, CA 94305

[2]Department of Chemistry, Stanford University, Stanford, CA 94305

[3]ChEM-H Institute, Stanford University, Stanford, CA 94305

*Corresponding Author: herschla@stanford.edu, (650) 723-9442

Table of Contents

1. **Figure S1.** Secondary structure of DNA constructs S2
2. **Figure S2.** pH-dependent fluorescence change S3
3. **Figure S3.** Representative proton binding assay data S4
4. **Figure S4.** Charge density and ion release S5-6
5. **Figure S5.** Electrostatic potentials around DNA S7-8
6. **Figure S6.** CD spectra of $24bp^{AC}$ S9
7. **Figure S7.** Test for specific salt effects S10
8. **Figure S8.** Wobble pair formation S11
9. **Tables S1-5.** Individual log K_A values S12-14
10. **Table S6-7.** Parameters for linear salt dependences S15
11. **Methods** (PB calculations and CD) S16-17
12. **References.** S18

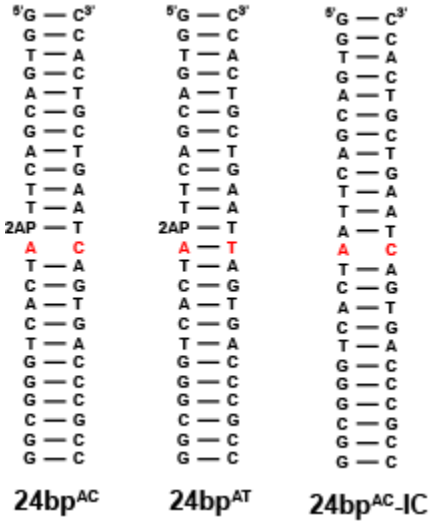

Figure S1. Secondary structure of DNA constructs used in this study. The sequence in red indicates A•C mismatch or AT control. 24bp^{AC}-IC is the construct used in ion-counting experiments. Each strand has 23 phosphoryl groups, with 5' and 3' hydroxyl groups, corresponding to an overall charge of -46 for each duplex.

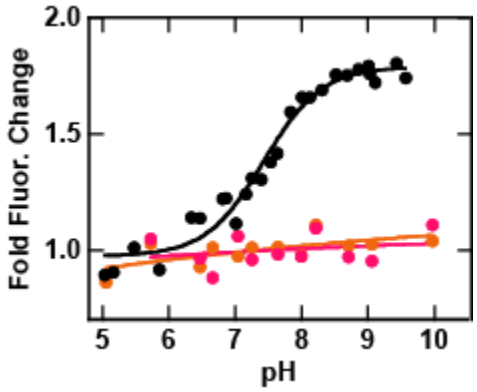

Figure S2. pH-dependent fluorescence change of 2AP in three DNA constructs: 24bp^{AC} (black); 24bp^{AT} (orange); and a single-stranded oligo (magenta). Sequences are given in Fig. S1, with the single-stranded oligo corresponding to the 2AP-containing strand of 24bp^{AC}.

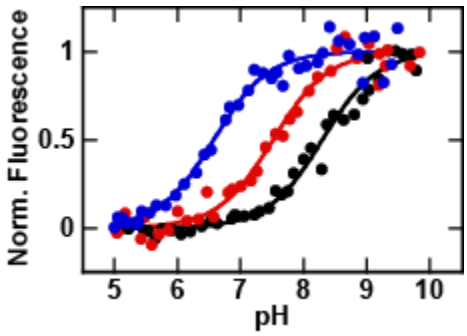

Figure S3. Representative proton binding assay data. The pH dependence of 24bp^{AC} fluorescence with K^+ at concentrations of 20 mM (black), 100 mM (red), and 1000 mM (blue). The data were fit with a single proton binding model (eq 2), giving log K_A = 8.30 ± 0.05, 7.52 ± 0.06, and 6.58 ± 0.06, respectively.

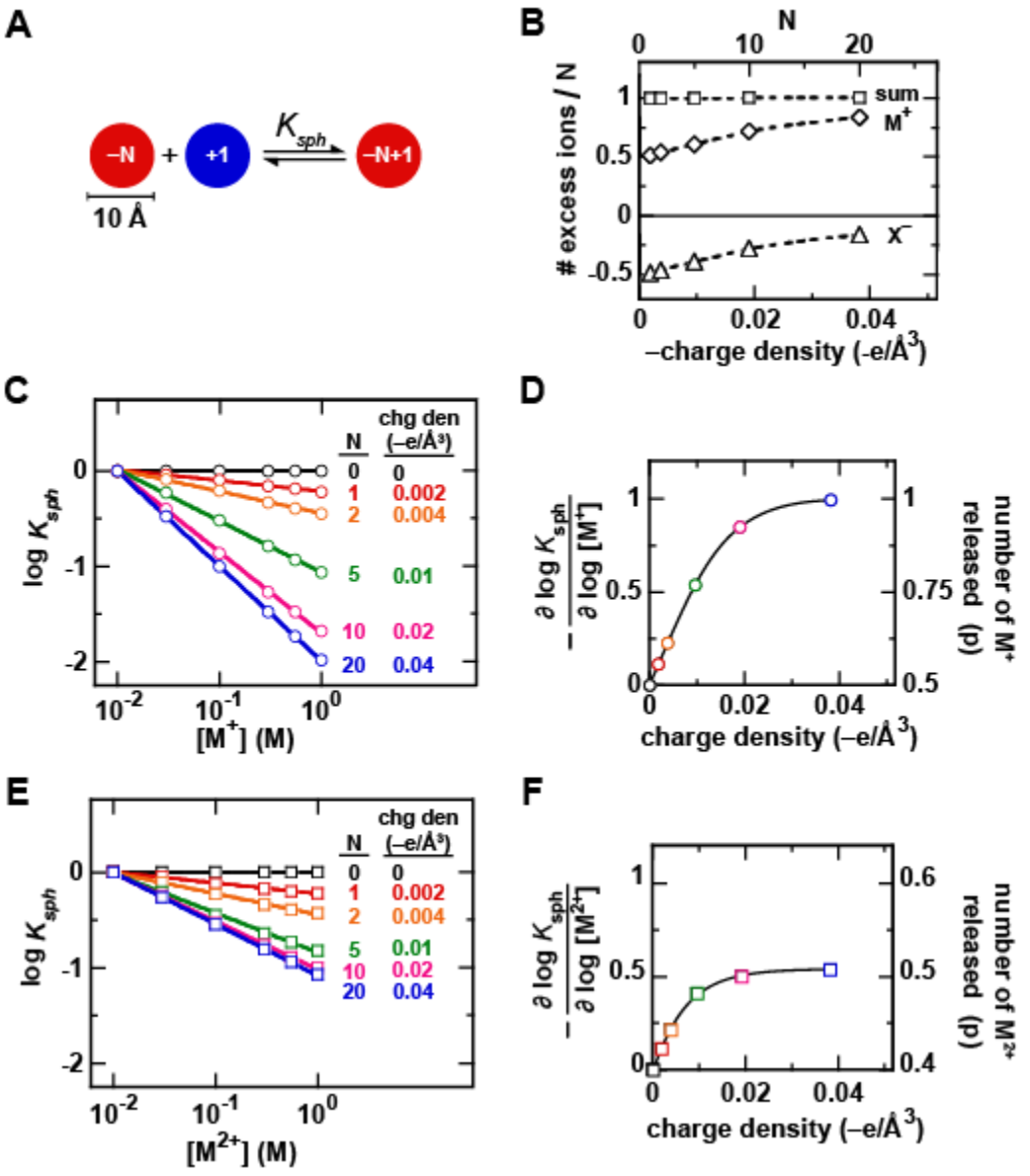

Figure S4. Poisson-Boltzmann (PB) predictions of the ligand association equilibrium as a function of the charge density of ligand-binding molecule and salt concentration. (A) A model of association (K_{sph}) between a negatively charged sphere (–N) and a positive point charge (+1). The diameter of the sphere is 10 Å. (B) Predictions for the composition of the ion atmosphere surrounding the free negatively charged sphere as a function of the sphere charge density. The

number of excess cations per the charge of the sphere (N) is represented by diamonds, the excess anions by triangles, and the sum of the cation and anion excess is shown with squares and agrees with the expectation for charge neutrality;[1,2] i.e., the sum ions is equal to the charge of the sphere. (C) Predicted monovalent salt dependences of the association constant for spheres of increasing charge density ('chg den'). (D) The influence of charge density on the salt dependence of association, i.e., the slopes of the lines plotted in part C. Colors of points correspond to N values and charge densities from part C. (E and F) As in parts (C) and (D) but for salts of divalent cations.

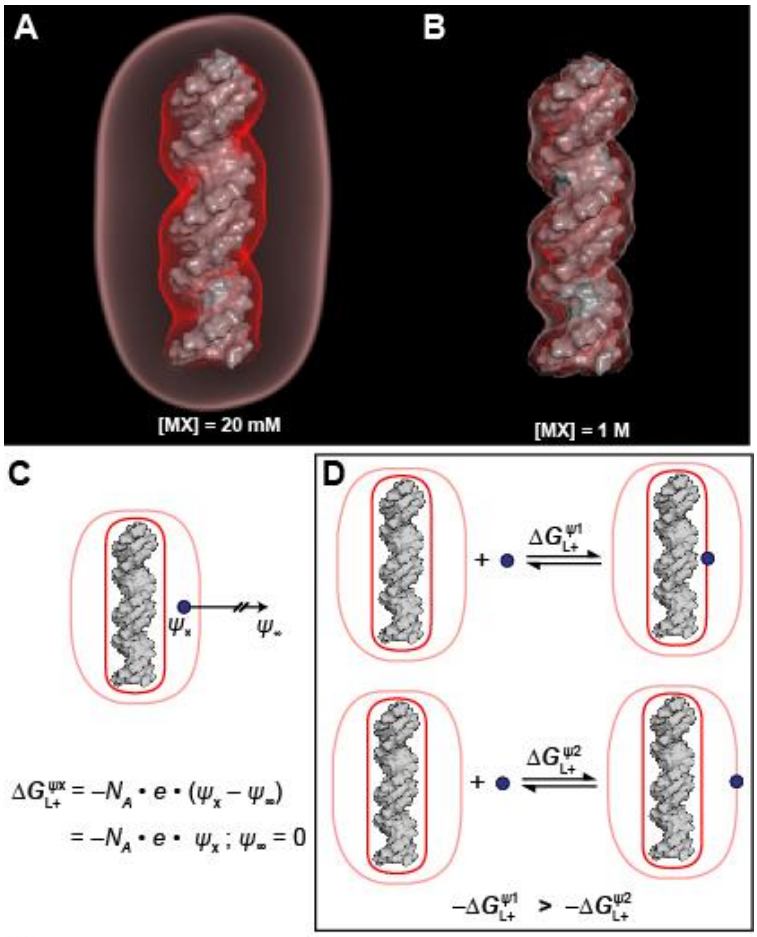
A
B
[MX] = 20 mM
[MX] = 1 M
C
D
ψ_x
ψ_∞
$\Delta G_{L+}^{\psi x} = -N_A \cdot e \cdot (\psi_x - \psi_\infty)$
$= -N_A \cdot e \cdot \psi_x ; \psi_\infty = 0$
$\Delta G_{L+}^{\psi 1}$
$\Delta G_{L+}^{\psi 2}$
$-\Delta G_{L+}^{\psi 1} > -\Delta G_{L+}^{\psi 2}$
E
0 10 20 30
r (Å)
F
[K+] (M)
0.02
0.1
1.0
$-\psi$ (mV)
300
200
100
0
0 10 20 30
r (Å)
G
PB
4.0 Å
5.0 Å
6.0 Å
$-\psi$ (mV)
300
250
200
150
100
50
10^{-2} 10^{-1} 10^{0}
[K+] (M)

Figure S5. Poisson-Boltzmann calculations of electrostatic potential. (A) The electrostatic potential surrounding a model of B-DNA in 20 mM monovalent salt is shown with isocontours at -25 mV (pink) and -100 mV (red). (B) Same as part A but with 1 M salt. (C) The energy of attraction of a positively charged ligand (L^+, blue sphere) to a nucleic acid is equal to the work required to move the charged ligand from near the nucleic acid with potential ψ_x to a position infinitely distant from the nucleic acid where the potential, ψ_∞, is defined as zero. N_A is Avogadro's number and e is the elementary charge. (D) The attraction of a positively charged ligand (L^+, blue sphere) to a nucleic acid varies with the electrostatic potential, with greater attraction for positions of higher potential (red versus pink electrostatic potential contour lines). (E) Positions for which the electrostatic potential was calculated using PB theory in part F. (F) Values for the electrostatic potential surrounding B-DNA at the positions indicated in part E, with r representing the distance from the center of the helix. The points at 4 Å are at the surface of the DNA, and all values of r less than 4 Å are within the surface (gray region) and therefore not well defined. (G) Comparison of electrostatic potentials calculated from experimental data for AH^+•C wobble formation (closed circles, data from Fig. 3) and the PB calculations of the potential at the DNA surface [open circle and lines; for r = 4.0 Å (blue), 5.0 Å (black) and 6.0 Å (red)].

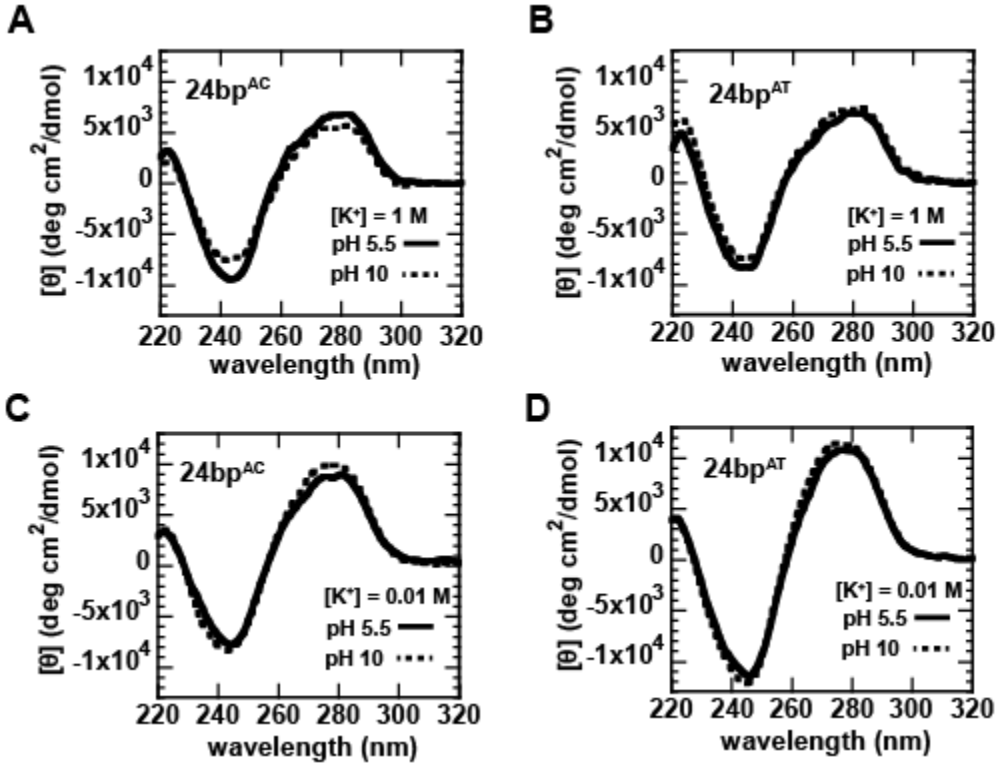

Figure S6. Circular dichroism (CD) spectra of 24bp^{AC}. Spectra were determined at 25 ºC at low and high pH. Molar ellipticity per base is reported. (A and B) At high salt ([K^+] = 1 M) spectra of 24bp^{AC} (A) and the fully base-paired construct 24bp^{AT} (B). (C and D) At low salt ([K^+] = 0.01 M) spectra of 24bp^{AC} (C) and the fully base-paired construct 24bp^{AT} (D).

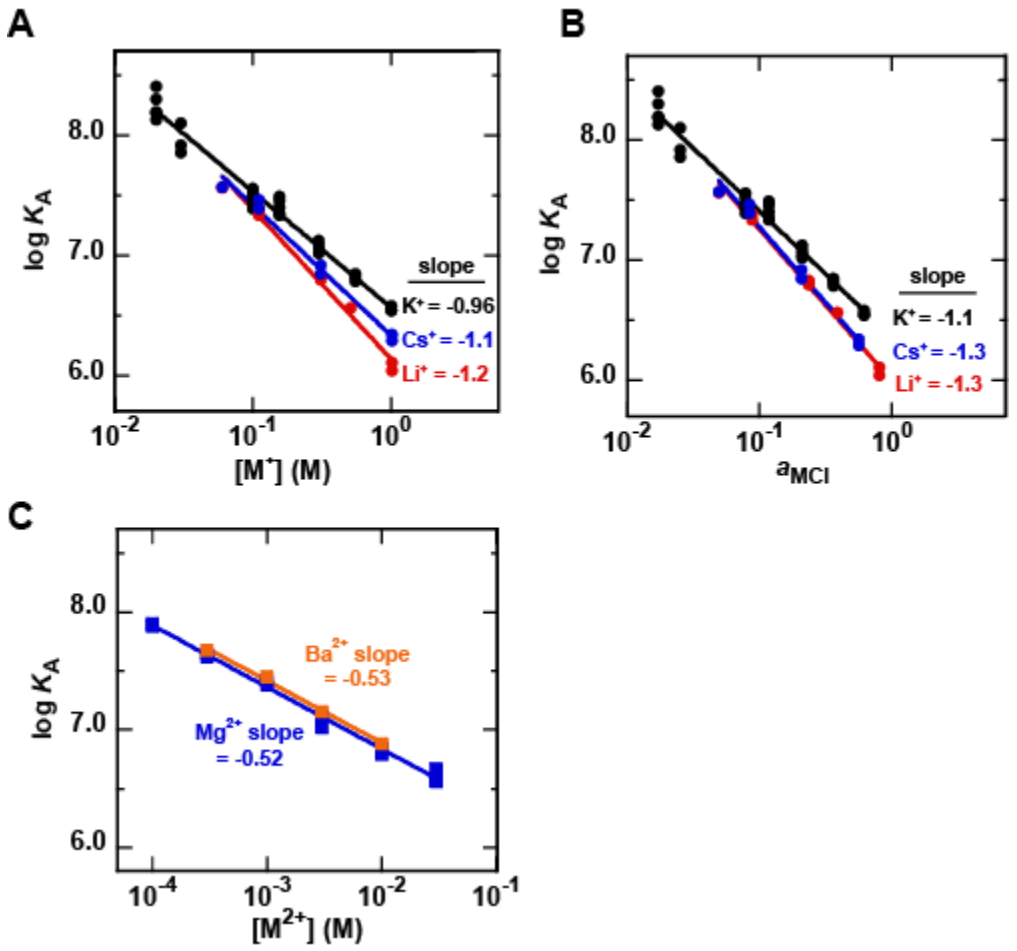

Figure S7. Dependence of the salt dependence of proton binding on cation identity. (A & B) The effect of monovalent cations of different size on proton association plotted as a dependence on cation concentration (A) and salt activity (B). The slopes are within or near within error of each other and the small differences are driven by effects at high salt concentrations where complex activity effects can arise. (C) The effect of different divalent cations on proton association. Individual log K_A values are given in Tables S2-5. Slopes parameters are given in Table S6 and 7.

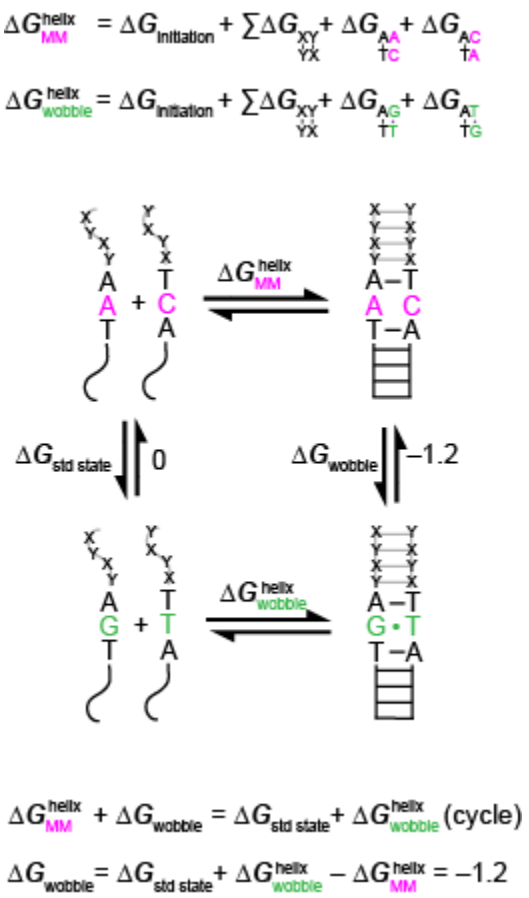

Figure S8. Framework for estimating the free energy of wobble pair formation. Contribution of an A•C mismatch and a G•T wobble to helix formation were previously determined within the nearest neighbor model (ΔG^{helix}_{MM} and $\Delta G^{helix}_{wobble}$, respectively).[3,4] The thermodynamic cycle links the formation of helices with mismatch and wobble pairs, so that completing the cycle provides a quantitative estimate for the free energy of formation of a wobble pair from a mismatch (ΔG_{wobble}). By using a G•T wobble pair, which is isosteric with an AH^+•C wobble pair,[5] ΔG_{wobble} represents the energy of forming an AH^+•C wobble without electrostatic contributions. Values have units of kcal/mol.

Table S1. Testing the salt dependence of buffer pH with pH-sensitive dyes

	pK_a of *p*-nitrophenol		**pK_a of Neutral Red**	
[K^+] (M)	Calculated[a]	Observed	Calculated[a]	Observed
0.01	7.11	7.11 ± 0.02		
0.1	7.04	6.96 ± 0.01		
0.3	7.00	7.14 ± 0.06	6.82	6.77 ± 0.02
1.0	7.00	6.88 ± 0.04	6.83	6.72 ± 0.02

[a]Salt dependence of literature reported pK_a values calculated using eq 1.[6,7]

Table S2. Proton Affinity of 24bp^{AC} in K^+ Solutions

[K^+] (M)	**α_{KCl}**[a]	**log K_A (25 °C)**[b]
0.02	0.017	8.13 ± 0.03
		8.19 ± 0.05
		8.19 ± 0.05
		8.30 ± 0.05
		8.41 ± 0.10
0.03	0.025	7.86 ± 0.08
		7.92 ± 0.06
		8.10 ± 0.05
0.10	0.077	7.44 ± 0.10
		7.47 ± 0.08
		7.39 ± 0.05
		7.52 ± 0.06
		7.56 ± 0.06
0.16	0.116	7.35 ± 0.05
		7.33 ± 0.05
		7.46 ± 0.04
		7.49 ± 0.02
		7.40 ± 0.05
0.30	0.206	7.08 ± 0.04
		7.12 ± 0.05
		7.05 ± 0.05
		7.02 ± 0.06
0.55	0.643	6.84 ± 0.06
		6.79 ± 0.06
		6.82 ± 0.04
1.00	0.604	6.54 ± 0.04
		6.58 ± 0.06
		6.54 ± 0.05

[a]Salt activity calculated using activity constants reported in Robinson and Stokes, 1959.[8] [b]Standard error reported.

Table S3. Proton Affinity of $24bp^{AC}$ in Li^+ Solutions

$[Li^+]$ (M)	$[M^+]$ (M) [a]	α_{LiCl} [b]	log K_A (25 °C) [c]
0.05	0.06	0.049	7.56 ± 0.04
0.10	0.11	0.087	7.34 ± 0.07
			7.39 ± 0.08
0.30	0.31	0.231	6.80 ± 0.03
			6.83 ± 0.04
0.50	0.51	0.377	6.56 ± 0.06
1.00	1.01	0.783	6.04 ± 0.07
			6.11 ± 0.03

[a]Monovalent salt concentration includes the 0.01 M K+ background. [b]Salt activity calculated using activity constants for LiCl (γ_{LiCl}) reported in Robinson and Stokes, 1959, where $\alpha_{LiCl} = \gamma_{LiCl}[M^+]$.[8] [c]Standard error reported.

Table S4. Proton Affinity of $24bp^{AC}$ in Cs^+ Solutions

$[Cs^+]$ (M)	$[M^+]$ (M) [a]	α_{CsCl} [b]	log K_A (25 °C) [c]
0.05	0.06	0.049	7.57 ± 0.06
0.10	0.11	0.082	7.39 ± 0.10
			7.46 ± 0.08
0.30	0.31	0.202	6.85 ± 0.04
			6.92 ± 0.04
1.00	1.01	0.549	6.29 ± 0.07
			6.34 ± 0.08

[a]Monovalent salt concentration includes the 0.01 M K+ background. [b]Salt activity calculated using activity constants for CsCl (γ_{CsCl})reported in Robinson and Stokes, 1959, where $\alpha_{CsCl} = \gamma_{CsCl}[M^+]$.[8] [c]Standard error reported.

Table S5. Proton Affinity of 24bp^{AC} in Mixed K^+/Mg^{2+} Solutions

	log K_A (25 °C)[a]		
[Mg^{2+}] (mM)	[K^+] = 20 mM	[K^+] = 160 mM	[K^+] = 300 mM
0	8.13 ± 0.03	7.35 ± 0.05	7.08 ± 0.04
	8.19 ± 0.05	7.33 ± 0.05	7.12 ± 0.05
	8.19 ± 0.05	7.46 ± 0.04	7.05 ± 0.05
	8.30 ± 0.05	7.49 ± 0.02	7.02 ± 0.06
	8.41 ± 0.10	7.40 ± 0.05	
0.1	7.88 ± 0.05	7.42 ± 0.03	7.09 ± 0.04
	7.90 ± 0.07	7.43 ± 0.03	
		7.28 ± 0.04	
0.3	7.65 ± 0.03	7.40 ± 0.05	7.01 ± 0.04
	7.62 ± 0.02	7.42 ± 0.03	
		7.29 ± 0.04	
1.0	7.42 ± 0.04	7.35 ± 0.03	7.07 ± 0.05
	7.38 ± 0.04	7.28 ± 0.03	
		7.31 ± 0.07	
1.8		7.18 ± 0.02	
3.0	7.12 ± 0.04	7.09 ± 0.03	6.97 ± 0.06
	7.02 ± 0.05	7.16 ± 0.02	
		7.09 ± 0.03	
		7.09 ± 0.04	
6.0		6.97 ± 0.02	
10	6.85 ± 0.03	6.92 ± 0.02	6.79 ± 0.07
	6.79 ± 0.05	6.91 ± 0.02	6.75 ± 0.05
	6.83 ± 0.03	6.82 ± 0.08	
		6.84 ± 0.05	
18		6.74 ± 0.03	
30	6.59 ± 0.03	6.59 ± 0.03	6.54 ± 0.05
	6.56 ± 0.04	6.61 ± 0.02	
	6.58 ± 0.03	6.69 ± 0.04	
	6.67 ± 0.06	6.58 ± 0.04	

[a]Standard error reported.

Table S6. Linear Parameters of Monovalent Cation-Dependent Proton Association (log K_A vs. log [cation]) for $24bp^{AC}$

Cation	**Bkgd** $[K^+]$ (mM)	**Slope**[a] ($\log K_A/\log[M^+]$)	**Intercept**[a] ($\log K_A$ at $[M^+]$=1M)	**Slope**[a] ($\log K_A/\log a_{MCl}$)	**Intercept**[a] ($\log K_A$ at a_{MCl}=1)
K^+	NA	-0.96 ± 0.03	6.55 ± 0.03	-1.06 ± 0.03	6.33 ± 0.03
Li^+	10	-1.25 ± 0.06	6.13 ± 0.04	-1.27 ± 0.05	5.98 ± 0.04
Cs^+	10	-1.08 ± 0.05	6.33 ± 0.04	-1.26 ± 0.06	6.00 ± 0.06

[a]Standard error reported.

Table S7. Linear Parameters of Mg^{2+}-Dependent Proton Association (log K_A vs. log $[Mg^{2+}]$) for $24bp^{AC}$

DNA	Bkgd $[K^+]$ (mM)	**Slope**[a] ($\log K_A/\log[Mg^{2+}]$)	**Intercept**[a] ($\log K_A$ at $[Mg^{2+}]$=1M)
$24bp^{AC}$	20	-0.52 ± 0.01	5.79 ± 0.03
$24bp^{AC}$	160	-0.49 ± 0.03	5.89 ± 0.06
$24bp^{AC}$	300	-0.48 ± 0.07	5.81 ± 0.07

[a]Standard error reported.

Methods

PB calculations with spheres

A sphere was defined with a 5 Å radius and an integer charge (-N, -N+1, and +1). The PB equation was numerically solved for each sphere at varying monovalent and divalent salt concentrations using the Adaptive Poisson-Boltzmann Solver (APBS) on a 482 x 482 x 562 Å grid with a 2.5 Å grid spacing and ion size equal to 2 Å.[9] The external dielectric was set at 78.54, typical of water at 25 ºC, and the internal dielectric was 2.0. The number of ions associated with the sphere was computed by integrating the excess ion density using eq 4.

The dependence of log K_s on salt concentration was calculated from the above values with use of Scheme S1.

Scheme S1

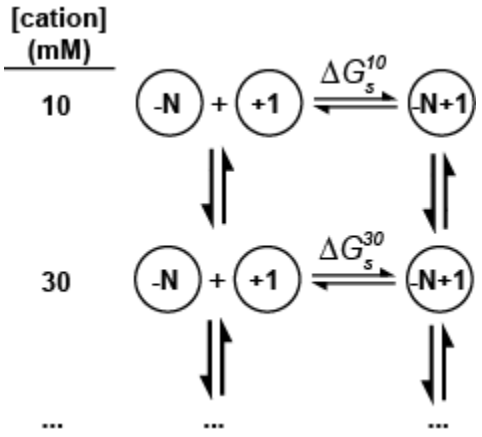

At each salt condition, ΔG_s is the difference in charging energy (ΔG_{ch}, obtained from APBS) of the product and the reactants (eq S1).

$$\Delta G_s = \Delta G_{ch}^{-N+1} - (\Delta G_{ch}^{-N} + \Delta G_{ch}^{+1}) \quad \text{(S1)}$$

The reaction with a cation concentration of 10 mM was used as a standard state, such that log K_s at cation concentration x was calculated using eq S2.

$$\log K_s^x = -\frac{(\Delta G_s^x - \Delta G_s^{10})}{2.3RT} \quad \text{(S2)}$$

PB calculations of electrostatic potential

The electrostatic potential was calculated by PB theory as implemented by APBS at defined positions relative to the molecular model of 24bpAC (see Methods). To define these positions, small uncharged spheres (radius = 0.25Å) were positioned on a line at the middle of and perpendicular to the helix axis, emanating through the major groove; these spheres were placed 0, 4, 6, 8, 12, 16, 20, and 30 Å from the center of the helix (see Fig. S5E). The electrostatic potential at the center of the spheres was calculated at 0.02, 0.1, and 1.0 M monovalent salt with APBS using the parameters listed above.

CD Measurements

Spectra were measured with 18 μM DNA in 1 mm quartz cells. The solutions was buffered with 5 mM potassium MES at pH 5.5 or potassium CAPS at pH 10.0. The absorbance of the buffer was subtracted.

References

(1) Bai, Y.; Greenfeld, M.; Travers, K. J.; Chu, V. B.; Lipfert, J.; Doniach, S.; Herschlag, D. *J. Am. Chem. Soc.* **2007**, *129* (48), 14981.

(2) Gebala, M.; Giambaşu, G. M.; Lipfert, J.; Bisaria, N.; Bonilla, S.; Li, G.; York, D. M.; Herschlag, D. *J. Am. Chem. Soc.* **2015**, *137* (46), 14705.

(3) Allawi, H. T.; SantaLucia, J. *Biochemistry* **1997**, *36* (34), 10581.

(4) Allawi, H. T.; SantaLucia, J. *Biochemistry* **1998**, *37* (26), 9435.

(5) Hunter, W. N.; Brown, T.; Anand, N. N.; Kennard, O. *Nature* **1986**, *320* (6062), 552.

(6) Jencks, W. P.; Regenstein, J. In *Handbook of Biochemistry and Molecular Biology*; CRC Press: Cleveland, 1976; pp 305–351.

(7) Walz, F. G.; Terenna, B.; Rolince, D. *Biopolymers* **1975**, *14* (4), 825.

(8) Robinson, R. A.; Stokes, R. H. *Electrolyte Solutions*, 2nd Rev. Ed.; Dover Publications: Mineola, NY, 2002.

(9) Baker, N. A.; Sept, D.; Joseph, S.; Holst, M. J.; McCammon, J. A. *Proc. Natl. Acad. Sci. U.S.A.* **2001**, *98* (18), 10037.